Collisional quenching of internally excited atoms and molecules at cold and ultracold temperatures

R. C. Forrey

Penn State University, Berks-Lehigh Valley College, Reading, PA 19610-6009

Abstract. Quantum mechanical calculations of collisional quenching cross sections and rate coefficients for various internally excited atoms and molecules at cold and ultracold temperatures are presented. The efficiencies of relaxation for vibrationally, rotationally, and electronically excited states are given and in each case the dominant decay mechanisms are discussed.

INTRODUCTION

During the past few years, major developments in the cooling and trapping of atoms and molecules [1] have provided a new probe of fundamental physics. Quantum mechanical effects play a dominant role at low energies, and collisional dynamics are very sensitive to the weak intermolecular forces between the atoms and molecules. Although translational temperatures typically reach into the milli-Kelvin range or below, the internal energy may be very hot by comparison. Therefore, the exchange of internal energy during a collision is an important issue in cold and ultracold physics. Here, we discuss several examples of collisional quenching of internally excited atomic and molecular states at low temperatures.

ELECTRONIC QUENCHING

The collisional quenching of electronic excitations in the interaction of two metastable hydrogen atoms has been investigated at thermal energies [2, 3]. Potential energy curves have been computed that correlate to pairs of $n = 2$ hydrogen atoms at large interatomic separation [4]. These calculations form the foundation for our continued research on metastable hydrogen at cold and ultracold temperatures [5]. Electronic quenching may occur as a consequence of excitation transfer and ionization. Here, we discuss the importance of ionization as a quenching mechanism in the interaction of two H(2s) atoms.

Excitation transfer and ionization occur through the accumulation of differences in phase in the scattering on two potential curves $V_\pm$. The potentials have imaginary components due to the autoionizing channels; this will give rise to ionization loss that may be strong at ultracold temperatures. At thermal energies, the scattering and ionization cross sections are given by

$$\sigma_{if} = \frac{\pi}{k^2}\sum_{l=0}^{\infty}(2l+1)\left|S_{if}^{(l)} - \delta_{if}\right|^2 \tag{1}$$

$$\sigma_{ionize} = \frac{\pi}{k^2}\sum_{l=0}^{\infty}(2l+1)\left[1 - A_l^2\right] \tag{2}$$

$$A_l^2 = \sum_f |S_{if}^{(l)}|^2 = \tfrac{1}{2}\left(|A_l^+|^2 + |A_l^-|^2\right) \tag{3}$$

where $S_{if}^{(l)}$ is the scattering matrix connecting the initial and final channels for partial wave l. The absorption factors $A_l^\pm$ are defined with respect to the potentials. Degenerate perturbation theory may be used to show that the potentials have the long-range form [3]

$$V_\pm(R) \sim \frac{l(l+1)}{2\mu R^2} \pm \frac{C_3}{R^3}\,. \tag{4}$$

Ionization may occur when the translational energy is greater than the potential energy barrier, which can be determined by differentiating $V_\pm$ with respect to R and setting to zero. The absorption factor A_l^- then behaves like a step function centered at

$$l = [54\mu^3 C_3^2 E]^{1/6}\,. \tag{5}$$

Equation (5) predicts that the steps will be located at l equal to 52, 35, 24, and 16 for energies equal to 10^{-3}, 10^{-4}, 10^{-5}, and 10^{-6} atomic units respectively. Fig. 1 shows a plot of A_l^2 as a function of l obtained using the full molecular potentials [4]. The steps are located as predicted above. The plot shows that the absorption factor is equal to one-half before reaching the location of the step. This is because $V_+(R)$ prevents the atoms from reaching short distances where autoionization can

CP680, *Application of Accelerators in Research and Industry: 17th Int'l. Conference*, edited by J. L. Duggan and I. L. Morgan

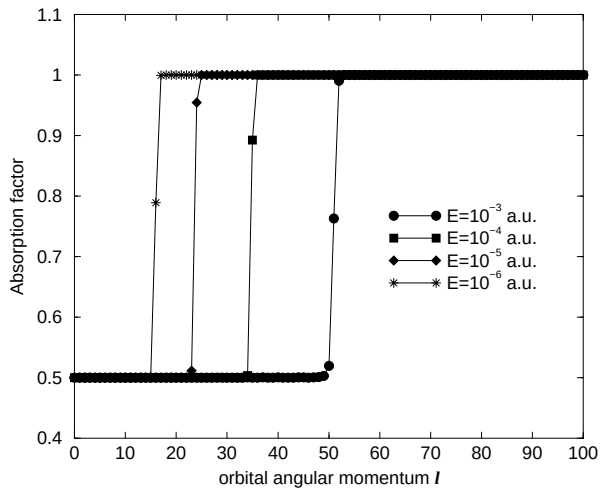

FIGURE 1. Absorption factor resulting from ionization.

take place. Therefore, $A_l^+ = 1$ for all l and equation (3) provides the factor of one-half. Equation (5) may be used in equation (2) to obtain the estimate

$$\sigma_{ionize} \approx \frac{3\pi}{2}\left(\frac{C_3}{2E}\right)^{2/3} \tag{6}$$

which equals $23.3E^{-2/3}$ for $C_3 = 22$ as derived in [3]. This estimate agrees with a numerically exact scattering calculation to within a few percent [3].

VIBRATIONAL QUENCHING

The collisional quenching of molecular vibrations has been investigated for homonuclear [6] and heteronuclear diatomic molecules [7]. In Fig. 2, we show the quenching rate coefficients for He collisions with $H_2(v, j = 0)$ where v, j are the respective vibrational and rotational quantum numbers. As the translational temperature is decreased, each vibrational level has a rate coefficient that reaches a minimum value around 10 K before increasing to the asymptotic value as required by Wigner's threshold law. A minimum value generally occurs when the temperature is comparable to the well-depth of the van der Waals potential between the collision partners. As temperature is decreased further, the attractive van der Waals force accelerates the collision into the strong interaction region resulting in an increased quenching rate coefficient. The rate coefficients increase systematically with increasing vibrational quantum number v and are about three orders of magnitude larger for $v = 10$ than for $v = 1$. This is presumably due to the increasing size of the molecule as the stretching is increased which causes an increased effective area for the collision to occur.

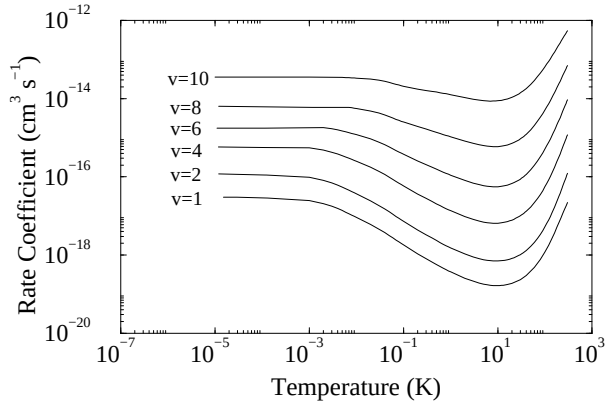

Source: Phys. Rev. Lett. 80, 3224 (1998)

FIGURE 2. Rate coefficients for the vibrational quenching of H_2 in collisions with ^{3}He.

The smooth behavior in the quenching cross sections and rate coefficients may be altered by the presence of shape resonances, and the systematic increase in the rate coefficients with v may be altered by the presence of a bound state near the zero-energy threshold. This is the case for He collisions with CO molecules [7]. The van der Waals well in the potential supports several shape resonances that influence the quenching cross sections at energies less than the well depth. A Feshbach resonance in the $j = 1$ level of the $v = 1$ manifold provides a dramatic influence on the quenching rate coefficients in the limit of zero temperature. This is shown in Fig. 3 where the rate coefficients are plotted versus temperature for $j = 0$ and $j = 1$.

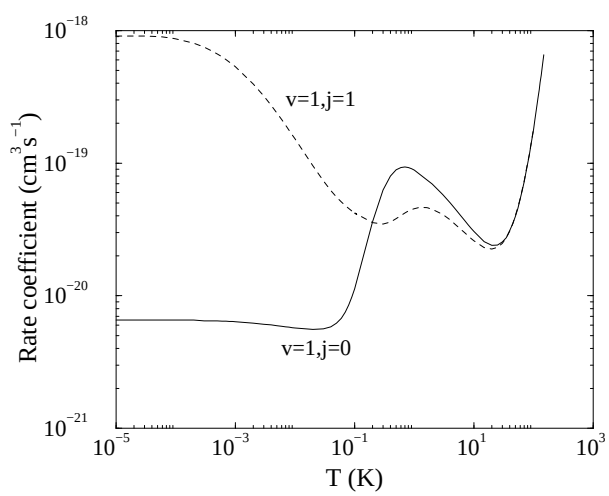

Source: J. Chem. Phys. 113, 621 (2000)

FIGURE 3. Rate coefficient for the vibrational quenching of CO in collisions with ^{4}He.

ROTATIONAL QUENCHING

Experimental schemes to produce diatomic molecules in highly excited rotational states have been proposed [8, 9] and recently realized [10]. The results of these experiments may have important implications for both gas phase and surface physics and chemistry [10]. The collisional quenching of such rotationally hot states has been investigated for hydrogen and oxygen molecules [11, 12]. As the translational kinetic energy is reduced, the total quenching cross section decreases sharply for specific channels where quasiresonant vibration-rotation (QRVR) transitions are no longer energetically allowed. This effectively stablilizes the so-called "super rotors" against collisional quenching. This is demonstrated in Fig. 4 where the ratio of total inelastic to elastic cross section is plotted versus translational energy for $H_2(v, j)$ collisions with He. The sudden drop in σ_{in}/σ_{el} for the $j = 22$ state may be easily understood. At translational energies above the location of the step [between 10 and 200 cm^{-1} for the data shown in the figure], the $j = 22$ level has an open QRVR channel available, allowing the super rotor to lose its rotation via the highly efficient and specific $\Delta j = -2\Delta v$ transition. As the energy is lowered, the QRVR transition for $j = 22$ becomes energetically forbidden and the total inelastic cross section is reduced by about five orders of magnitude. The $j = 20$ and $j = 24$ super rotors have QRVR transitions that remain open in the limit that the translational energy goes to zero. As shown in Fig. 4, there is no sudden drop in σ_{in}/σ_{el} for these super rotors as the temperature is decreased. Therefore, the $j = 20$ and $j = 24$ super rotors will be fragile and the $j = 22$ super rotor will be stable against collisional decay at cold and ultracold temperatures.

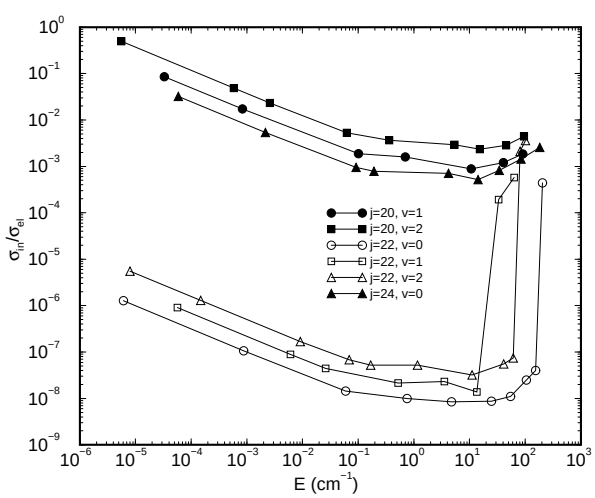

FIGURE 4. Ratio of total inelastic to elastic cross section for ^{3}He+H_2 collisions as a function of translational energy.

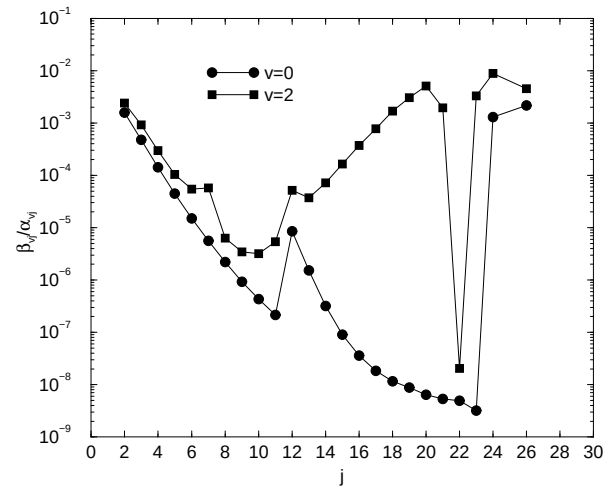

Source: Phys. Rev. A 66, 023411 (2002)

FIGURE 5. Ratio of imaginary to real part of the complex scattering length as a function of rotational level for collisions of ^{4}He with $H_2(v, j)$ in the limit of zero temperature.

Fig. 5 shows the ratio of imaginary to real part of the complex scattering length as a function of rotational level for collisions of He with $H_2(v, j)$ in the limit of zero temperature. The imaginary part β_{vj} is a measure of the total inelasticity and includes contributions from all possible de-excitation channels. The structure in the rotational level distributions is due to the availability of open QRVR transitions. For $v = 0$, the system cannot undergo $\Delta v = -1$ transitions, so the distributions are asymmetric with respect to the QR j-values ($j = 10$ and $j = 22$). For $v > 0$, the system can make upward or downward QRVR transitions, so the distributions are symmetric with respect to the QR j-values. In both cases, the $j = 22$ level is stable against collisional de-excitation.

The dependence of the total inelastic cross section on the anisotropy of the potential energy surface has been studied. Light diatomic systems with small long-range anisotropy generally allow the most stable rotationally excited states when the QRVR channels are closed. This is due to the exponential decay of the rate coefficients for pure rotational transitions as the energy gap between the initial and final state is increased [13, 14]. Fig. 6 compares the ratios β_j/α_j for hydrogen and oxygen molecules under the condition that vibrational transitions are not allowed. The rotational energy level spacings for oxygen molecules are much smaller than for hydrogen molecules. Therefore, the oxygen molecule can support higher rotational levels ($j \approx 180$) before experiencing centrifugal dissociation. Fig. 6 shows calculations for $j < 45$. Although it was not possible to obtain converged quantum mechanical results for larger rotational levels, it is clear that super rotors made of oxygen would be

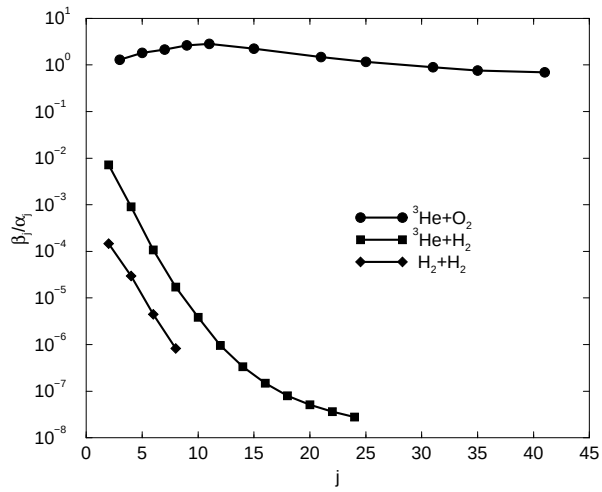

Source: Phys. Rev. A 66, 023411 (2002)

FIGURE 6. Ratio of imaginary to real part of the complex scattering length for various systems. The calculations were constrained such that vibrational transitions were not allowed.

very fragile compared to those of hydrogen. This is due to the anisotropy in the potential energy surface. Heavier systems with large anisotropy have rate coefficients for pure rotational transitions that fall off more slowly with energy gap, allowing more efficient relaxation even when QRVR transitions are closed. The long-range anisotropy in the potential energy surface may be estimated using the relation [15]

$$V_L(R,\gamma) \approx -\frac{C_6}{R^6}\left[1+\frac{\alpha_{||}-\alpha_{\perp}}{\alpha_{||}+2\alpha_{\perp}}P_2(\cos\gamma)\right] \qquad (7)$$

where $\alpha_{||}$ and $\alpha_{\perp}$ are the components of the diatomic polarizability that are parallel and perpendicular to the internuclear axis. Strong anisotropy may destroy any possibility for cooling and trapping. Hydrogen molecules would offer the best stability against collisional decay, however, they would also be the most difficult to rotate because the magnitude of $\alpha_{||}-\alpha_{\perp}$ is what allows the diatomic molecules to be spun to such high rotational levels [10]. In a practical application, it may be desirable to sacrifice some collisional stability in order to gain other advantages. For example, a molecule possessing a magnetic dipole moment would allow a trapping scheme that is analogous to the atomic case. If the molecule retains enough collisional stability and allows enough state selectivity (e.g. the $j = 22$ result of Fig. 5), then it is conceivable that evaporative cooling could be used in an effort to reach Bose-Einstein condensation.

CONCLUSION

Translationally cold atoms and molecules are sensitive to weak forces. As a result, experiments can now provide information about atomic and molecular interactions at an unprecedented level of detail. In order to analyze and interpret this information and to provide guidance and motivation for new experiments, it is necessary to perform theoretical studies at the same level of detail. In this paper, we have discussed several examples of collisional quenching of internally excited atomic and molecular states at low temperatures. Results of quantum mechanical calculations have been given for collisional quenching cross sections and rate coefficients, together with a discussion of the dominant decay mechanisms.

ACKNOWLEDGMENTS

I would like to acknowledge and thank my collaborators N. Balakrishnan, R. Cote, A. Dalgarno, P. Froelich, S. Jonsell, V. Kharchenko, and A. Saenz. This work has been supported by the National Science Foundation grant No. PHY-0070920.

REFERENCES

1. see J. Weiner, V. S. Bagnato, S. Zilio, and P. S. Julienne, Rev. Mod. Phys. **71**, 1 (1999).
2. X. Urbain, A. Cornet, and J. Jureta, J. Phys. B **25**, L189 (1992).
3. R. C. Forrey, R. Cote, A. Dalgarno, S. Jonsell, A. Saenz, and P. Froelich, Phys. Rev. Lett. **85**, 4245 (2000).
4. S. Jonsell, A. Saenz, P. Froelich, R. C. Forrey, R. Cote, and A. Dalgarno, Phys. Rev. A **65**, 042501 (2002).
5. Our calculations are motivated by ongoing experiments in the lab of T. J. Greytak and D. Kleppner at MIT.
6. N. Balakrishnan, R. C. Forrey, and A. Dalgarno, Phys. Rev. Lett. **80**, 3224 (1998).
7. N. Balakrishnan, A. Dalgarno, and R. C. Forrey, J. Chem. Phys. **113**, 621 (2000).
8. J. Karczmarek, J. Wright, P. Corkum, and M. Ivanov, Phys. Rev. Lett. **82**, 3420 (1999).
9. J. Li, J. T. Bahns, and W. C. Stwalley, J. Chem. Phys. **112**, 6255 (2000).
10. D. M. Villeneuve, S. A. Aseyev, P. Dietrich, M. Spanner, M. Y. Ivanov, and P. B. Corkum, Phys. Rev. Lett. **85**, 542 (2000).
11. R. C. Forrey, Phys. Rev. A **63**, 051403 (2001).
12. R. C. Forrey, Phys. Rev. A **66**, 023411 (2002).
13. T. A. Brunner and D. E. Pritchard, Adv. Chem. Phys. **50**, 589 (1982).
14. A. J. McCaffery, Z. T. Alwahabi, M. A. Osborne, and C. J. Williams, J. Chem. Phys. **98**, 4586 (1992).
15. A. D. Buckingham, Adv. Chem. Phys. **12**, 107 (1967).